iForest
Biogeosciences and Forestry

Research Article
doi: 10.3832/ifor4983-019
vol. 19, pp. 283-291

Improving the mechanized logging safety on steep slopes through the analysis of dynamic behavior of harvester rope anchor systems

Alexander Lagerev [(1)], Igor Lagerev [(2)], Anna Makulina [(3)]

Mechanized logging on steep slopes using forestry machines equipped with winch-rope anchor systems to ensure equipment stability and safe operation is becoming increasingly popular. The parameters that characterize the dynamic behavior of both the harvester and the rope anchor system are crucial to the operational efficiency of the anchor system. The purpose of this study is to create a comprehensive mathematical 12-mass model for the dynamic system "harvester - manipulator - anchor system - natural anchor - log - soil". The developed model combines all the key components of the system and enables assessment of their mutual influence on the quantitative parameters of the dynamic processes occurring in the system. The model includes 34 generalized coordinates that describe the displacement of the center of mass of each component of the harvester during its operations for felling trees and moving logs to the laying place. To construct a system of equations of motion characterizing the dynamics of the simulated system, an approach based on Lagrange equations of the 2nd kind was used. The model allows for analyzing the influence of the harvester's design and operating parameters, and of the physical and mechanical properties of the ground, on the harvester load with a manipulator and on the structural elements of the anchor system. To demonstrate the model's functionality, a specific 6-wheeled harvester weighing 20 tons was chosen as the study object while operating on slopes with a steepness ranging from 50% to 100%. The variable inertial loads on the manipulator from the displaced log cause oscillations in the tensile force of the anchor rope. The maximum values of the force in the studied range of slope steepness increased from 19 kN to 72 kN, while the average values increased from 16 kN to 65 kN, with an increase of oscillation in the range 6-14 kN. The oscillation frequency remains constant throughout the log's motion, as it is determined by the geometric dimensions of the structural elements in the simulated dynamic system.

Keywords: Oscillatory Processes, Modeling, Lagrange Equation, Dynamic Parameters, Dynamic Rope Tensile Force, Anchor Tree

Introduction

Natural forests suitable for logging are often found in challenging mountainous areas, with high-quality stands typically located on steep slopes (Visser & Stampfer 2015, Duka et al. 2025), making logging difficult (Aggestam et al. 2020). However, mechanized logging is currently being carried out in steep slope territories across several European countries (Italy, Croatia, Czech Republic, etc.), as well as in America (USA, Canada, Chile, etc.), Asia (Turkey, China, Korea, etc.), Australia, and New Zealand (Bont & Heinimann 2012, Naillon & Rappin 2019, Aggestam et al. 2020). Logging operations are only permitted in areas where the ground's slope is within the safe limits for operating logging machines. This maximum slope is defined by safety regulations for mechanized logging in various countries (Berkett & Visser 2012, Visser & Stampfer 2015). For example, current regulations in the province of British Columbia (Canada) restrict the safe use of land-based logging equipment on slopes not exceeding 40% (nearly 22 degrees – Mologni et al. 2018). Thus, the expansion of the possibilities for mechanized logging on steep slopes is directly related to improvements in the technical capabilities of forestry machines, which can increase the maximum inclination angles for safe operation.

Several approaches to solving this problem are known, for example, by optimizing the kinematic schemes of harvester manipulators (Lagerev et al. 2025) or introducing digital technologies based on artificial intelligence to optimize logging planning and execution within a cyber-physical system in accordance with the Forestry 4.0 concept (Humphrey et al. 2024). However, a promising approach is to incorporate additional technical devices into the harvester design to expand the capabilities of mod-

(1) Institute of Transport Technology and Control Systems, Russian University of Transport, Moscow, 127055 (Russia); (2) Rectorat, Kuban State Technological University, Krasnodar, 350072 (Russia); (3) Faculty of Physics and Mathematics, Academician I G Petrovskii Bryansk State University, Bryansk, 241036 (Russia)

@ Alexander Lagerev (ntv-brgu@yandex.ru)

Received: Sep 09, 2025 - Accepted: Mar 17, 2026

Citation: Lagerev A, Lagerev I, Makulina A (2026). Improving the mechanized logging safety on steep slopes through the analysis of dynamic behavior of harvester rope anchor systems. iForest 19: 283-291. – doi: 10.3832/ifor4983-019 [online 2026-07-28]

Communicated by: Rodolfo Picchio

ern forestry machines for safe operation on steep slopes.

One of the effective measures to prevent harvesters from rolling down the slope under their own weight is the use of rope anchor systems based on a traction winch mounted on the supporting frame of a forestry machine (Visser & Stampfer 2015, Naillon & Rappin 2019). Currently, both specialized harvesters with an initially installed winch and winch equipment kits are used to modify existing harvesters (Grim 2025). Using a rope winch allows forestry machines to be operated safely on steep support surfaces with slopes ranging from 60% to 100% (approximately 30 to 45 degrees – Berkett & Visser 2012). These slopes greatly exceed the maximum incline allowed by safety regulations for the safe operation of forestry equipment without an anchor-rope winch. A theoretical assessment of the stability of forestry machines equipped with a winch anchoring system on steep slopes was conducted by Sessions et al. (2017). The developed mathematical model enables assessment of the impact of equipment size and technical characteristics, soil properties, and site conditions on acceptable slopes and ground pressure.

Nowadays, rope anchor systems based on a traction winch can be dynamic or static (Leschinsky et al. 2015, Holzfeind et al. 2020). In dynamic anchor systems, a winch is attached to heavy mobile equipment, such as a bulldozer, tractor, or excavator, which acts as an artificial anchor and synchronizes the winch's operation with the harvester movement. In contrast, in static anchor systems, the winch is attached to the harvester frame, and a tree or stump at the top of the slope serves as a natural retaining anchor due to its strength and resistance to uprooting (Green et al. 2020). The results of experimental studies on the selection of such an anchor tree have been presented in Marchi et al. (2019). Lyons et al. (2020) explored the use of three stumps as an anchoring option to increase the bearing capacity of a natural anchor, in case one stump alone is not sufficient.

The positive impact of rope anchor systems based on a retaining winch is evident not only in their ability to facilitate mechanized logging on extremely steep slopes, but also in various other operations. Kormanek et al. (2023), Machuga et al. (2024), and Belart et al. (2025) reported that rope anchoring for forest machinery also has a positive effect on soil and groundwater, due to a more favorable pressure distribution and reduced soil compaction. Moreover, the use of a retaining winch increases logging productivity on moderately steep slopes. However, on a very steep slope, an increase in the maximum load weight from using a winch does not offset the reduction in machine speed (Visser & Spinelli 2023). An increase in the reliability of these forest machines has also been reported (Kovác et al. 2023).

According to Di Fulvio et al. (2024), the further expansion of efficient and safe mechanized logging requires adapting forestry equipment to more severe operating conditions in areas with large permissible inclination angles of the support surface. This necessitates conducting a range of theoretical and practical studies to develop new systems, machines, and mechanisms capable of addressing this challenge (Wassermann 2018, McEwan et al. 2020).

Research on logging machines with rope anchor systems using retaining winches on steep slopes is primarily experimental, focusing on field observations of the static and dynamic behaviors of parameters related to harvester operation and their anchoring systems. For example, Holzleitner et al. (2018) developed an automated system to monitor tensile forces in anchor ropes enabling measurements at various stages of harvester and forwarder operation. Similar studies conducted by Mologni et al. (2018) on large forwarders moving along a slope showed higher tensile force in the anchor rope when moving upwards. Also, Mologni et al. (2021a, 2021b) considered dynamic anchoring systems in which a tracked excavator serves as a mobile anchor, showing higher tensile force values for the anchoring machine.

A comparative analysis of the results from the aforementioned studies reveals qualitative agreement. However, quantitative comparisons are infeasible due to significant differences in experimental conditions and insufficient details. Across all studies, there is significant variability in the tensile force of anchor ropes during forestry machinery operation, influenced by factors such as the operating stage and mode, the direction of machine movement, soil inclination angle, distance to the anchor, and other variables.

Understanding how the work processes affect the anchor system of a working harvester is essential in theoretical studies of the harvester's dynamic behavior, and ultimately to determine the safety of logging on steep slopes. Modern mathematical modeling methods, combined with high-performance computers, enable the creation of complex dynamic models of work processes that account for numerous significant quantitative parameters contributing to their formation, and the analysis of the degree and direction of their individual and combined influence.

To date, the dynamic behavior of a working harvester on a steep slope has been modeled using multi-mass models constructed using the Dalembert principle or Lagrange equations of the second kind. These models differ in the number of structural components of the harvester's design they account for, and in their approaches to accounting for the influence of the anchor rope. These models offer varying degrees of detail of the dynamic processes being studied. For example, Grigorev et al. (2022) considered multi-mass models of wheeled machines and skidding tractors operating on a slope that simulated machine vibrations in both longitudinal and transverse planes. Sessions et al. (2017) developed a multi-mass model of a tracked tractor to study the machine's traction capacity and the maximum permitted inclination angles. This is similar to the models developed by Papadopoulos & Sarkar (1997) and Naillon & Rappin (2019). The influence of the anchor rope was modeled using a stationary force. This approach did not account for oscillations in the anchor rope's tension, which could affect the machine's dynamic behavior. However, the need to consider these oscillations was demonstrated during experimental studies of harvesters in field conditions (Holzleitner et al. 2018). Sun et al. (2020) proposed a mathematical model to study the dynamics of forest machines operating on slopes. The design of these machines includes special articulated mechanisms for leveling. Ismoilov et al. (2014), using the MSC/ADAMS software package, analyzed the dynamics of a wheeled, four-axle, articulated forwarder moving along a slope. Mergl & Kašpárek (2022) used the aforementioned software package to evaluate the effect of a manipulator on a forestry machine operating on slopes without an anchor rope. However, at present, no dynamic models are available to enable the quick assessment of rope tension for the development of control systems and the prevention of accidents (Visser et al. 2014).

The aim of this study is to create a comprehensive 12-mass mathematical model for the dynamic system "harvester - manipulator - anchor system - natural anchor - log - soil". The model developed combines all the key components of the system under study and enables assessing their mutual influence on the quantitative parameters of the dynamic processes occurring in the system. The basic principle for constructing a dynamic model was to represent a working harvester on a steep slope as a single object supported by a static rope anchor system, accounting for the individual characteristics of its structural components and the complex interactions among them.

Materials and methods

Dynamic mathematical model

The dynamic state of a harvester on a steep slope, anchored by a rope system to prevent uncontrolled movement, results from the interaction among several structural components. These components include the harvester itself, which is a self-propelled machine with equipment mounted on it, a manipulator mounted on the harvester's frame, an anchor system consisting of an anchor winch and an anchor rope, a movable log, and the natural anchor, which can be located on a tree or stump in the cutting area. The soil of the supporting surface also plays a role in this process. Considering the geometric and physical-mechanical characteristics of each component, as well as the varying nature of the load during moving logs from the cutting site to the temporary stacking site, we can perform a detailed analysis of the dynamic load on the harvester and its anchor system during operation.

Fig. 1 shows a dynamic mathematical model of the "harvester – manipulator - anchor system - natural anchor – log - soil" system, which implements this paradigm for a three-axle wheeled harvester with an uncut machine frame, using a suitable anchor tree as the natural anchor. The model allows for simulating the dynamics of a motionless harvester fixed on a slope using a single-branch anchor rope and moving logs from the cutting site to the temporary stacking site using a manipulator. Fig. S1 (in Supplementary material) shows a geometric model of the "harvester – manipulator - anchor system - natural anchor – log - soil" system corresponding to the model in Fig. 1.

When constructing a dynamic mathematical model, the following considerations were taken into account for its structural components. The metal structures of the harvester's frame have a length L_f and a width D_f. The frame consists of rigid rods characterized by linear weights g_f and the inertia moments of the sections EF_f. The total mass of the harvester M_h is the sum of the masses of its main structural elements, *i.e.*, frame, cabin, power plant, auxiliary equipment, wheel axle suspensions and wheels. The center of mass of the harvester is located at point $c.g_h$.

The manipulator provides the necessary movement of the harvester head and logs within the harvester's working area and has four degrees of freedom. Accordingly, it has four movable links, including a rotary column (link 1), a rotary boom (link 2), a rotary handle (link 3), and a translational telescopic link (link 4). These links are considered elastic rods with length L_i and a variable cross-sectional area along their length. They are characterized by their linear weights g_i and moments of inertia for bending in the vertical and transverse directions, denoted by EJ_{iv} and EJ_{ic}. The movements of the links in the manipulator are driven by hydraulic cylinders, with each cylinder moving one link. Based on the practice of dynamic analysis of multi-link manipulators (Ceccarelli 2008, Lagerev et al. 2014, Siciliano & Khatib 2016), the drive hydraulic cylinders can be considered as viscoelastic elements. Thus, the characteristics of the *i*-th hydraulic cylinder are described by the stiffness coefficient c_{hi} and the viscous resistance coefficient β_{hi} (Lagerev et al. 2014). The total mass of the manipulator M_m is the sum of the masses of all links and hydraulic cylinders. The center of mass of the manipulator is located at point $c.g_m$.

The metal structure of the anchor winch, including the drum, is considered as a set of interconnected elastic rods. It is characterized by the total weight M_w of the winch itself and the part of the anchor rope *F* that is wound around the drum, as well as the coefficient of stiffness in the longitudinal direction c_w. The center of mass of the anchor winch is located at point $c.g_w$.

The wheel axles of the harvester are considered as rigid rods that are connected to the frame by the same type of suspensions. In the vertical direction, the dynamic characteristics of suspensions are expressed by the stiffness coefficient c_s and viscous resistance coefficient β_s. Harvester wheels are considered as viscoelastic elements with a mass M_t. The center of mass of the *i*-th wheel is located at point $c.g_{ti}$. In accordance with the practice of analyzing the interaction of wheels of self-propelled multiaxial chassis with the support surface (Shoop 2001, Pracejka 2006), their dynamic characteristics are expressed by the stiffness coefficients of the tire material in the longitudinal (c_{tx}), radial (c_{ty}), and transverse (c_{tz}) directions of tire deformation, as well as the viscous resistance coefficients of the tire material in the specified directions β_{tx}, β_{ty}, and β_{tz}.

The anchor rope is considered a flexible thread with constant cross-section, diameter d_r, linear weight g_r, and stiffness coefficient c_r. The rope has a variable length depending on the distance from the anchor tree $L_r \in [L_{r,\ min};\ L_{r,\ max}]$ and, accordingly, a variable mass M_r. In the span between the anchor tree and the anchor winch, the rope has a natural static sag, the magnitude of which depends on the tensile force (Lagerev & Lagerev 2020). The center of mass of the anchor rope is located at point $c.g_r$.

The anchor tree is considered an elastic cantilever rod of variable cross-section with height L_{at}. The density ρ_{at} expresses its characteristics, the stiffness coefficient c_{at} and the viscous resistance coefficient β_{at} of wood (Placet et al. 2007). The mass of the anchor tree M_{at} is concentrated in the center of mass $c.g_{at}$ at a height H_{at} above the ground.

The soil of the support surface is considered as a viscoelastic medium. Its physical and mechanical properties depend on the type and condition of the soil. These properties are expressed by the coefficients of stiffness (c_{gr}) and viscous resistance (β_{gr}) in the vertical direction (Grigorev et al. 2022, Vereecken et al. 2016), as well as by the harvester's wheel slip, μ_{gr} (Machuga et al. 2024, Breinig et al. 2025). The dynamic model uses the kinetic coefficient of sliding, as when the harvester is running, there is constant, oscillating sliding of the braked wheels along the supporting surface, in accordance with a constant, oscillating change in the length of the anchor rope. In this dynamic model, the effects of soil compaction are not considered.

The Kelvin-Voigt model was used for all structural components as their viscoelastic representation (Meyers & Chawla 2009).

The system of motion equations

To construct a system of motion equations that characterize the dynamics of the six-component simulated system, an approach based on the Lagrange equations of the 2nd kind (Vinogradov 2000) was used. The model is characterized by a total of 34 degrees of freedom and correspond-

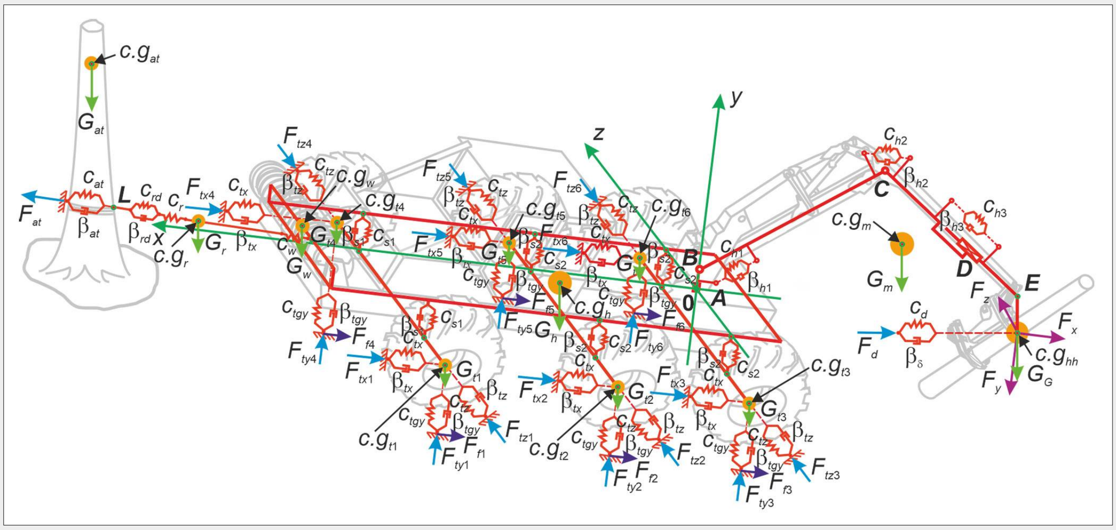

Fig. 1 - A dynamic mathematical model.

ing 34 generalized coordinates. These generalized coordinates are shown in Fig. S2 (Supplementary material) and represent linear and angular displacements of the center of mass of each component in the simulated system. These coordinates will be used in further calculations to determine the positions of the components.

In relation to the dynamic model under consideration, the system of Lagrange equations of the 2nd kind is expressed as (eqn. 1):

$$\frac{d}{d\tau}\left(\frac{\partial T}{\partial \dot{q}_i}\right)-\frac{\partial T}{\partial q_i}=Q_i, i\in[1;34] \quad (1)$$

where T is the total kinetic energy of the simulated system, q_i is the i-th generalized coordinate, $\dot{q}_i$ is the i-th generalized velocity, Q_i is the i-th generalized force.

The total kinetic energy T is the sum of the individual contributions of the kinetic energy of the simulated system's individual components: harvester (T_h), manipulator (T_m), harvester head together with the log (T_G), wheels (T_t), anchor winch (T_w), anchor rope (T_r), and anchor tree (T_{at}). It is expressed by eqn. 2:

$$\begin{aligned} T&=T_h+T_m+T_G+T_t+T_w+T_r+T_{at}\\ &=\frac{M_h+M_m+M_G+M_w}{2}\sum_{k=1}^{k=3}\dot{q}_k^{\,2}\\ &+\frac{J_{hx}}{2}\dot{q}_4^{\,2}+\frac{J_{hy}}{2}\dot{q}_5^{\,2}+\frac{J_{hz}}{2}\dot{q}_6^{\,2}+\frac{M_m+M_G}{2}\sum_{k=7}^{k=9}\dot{q}_k^{\,2}\\ &+\frac{M_G}{2}\sum_{k=10}^{k=12}\dot{q}_k^{\,2}+\frac{J_{Gz}}{2}\dot{q}_{13}^{\,2}+\frac{M_t}{2}\sum_{k=14}^{k=31}\dot{q}_k^{\,2}\\ &+\frac{M_w}{2}\dot{q}_{32}^{\,2}+\frac{M_r}{2}\sum_{k=33}^{k=34}\dot{q}_k^{\,2}+\frac{M_{at}}{2}\dot{q}_{35}^{\,2} \end{aligned} \quad (2)$$

where J_{hx}, J_{hy}, J_{hz} are the harvester inertia moments when rotating relative to the coordinate axes x, y, z, and M_G, J_{Gz} are the mass of the harvester head together with the log and the inertia moment when swinging relative to the coordinate axis z.

To determine the generalized forces Q_i corresponding to the generalized coordinates q_i, the algorithm described in Molotnikov & Molotnikova (2023) was used. This algorithm accounts for the effects of various forces used in the dynamic model of a six-component system. These forces include gravity, elasticity of system elements, resistance to sliding of wheels on the ground, and viscous resistance during deformation of system elements.

For each generalized force Q_i, the work sum δA of all forces taken into account in the geometric model of the system was determined on the generalized possible displacement δq_i, provided that 0 (zero) of the remaining generalized possible displacements are equal (eqn. 3):

$$\begin{aligned} \delta A&=\sum_i \delta A(M_i)+\sum_j \delta A(F_j)\\ &+\sum_k\left[\delta A(M_{tk})+\delta A(F_{txk})+\delta A(F_{tyk})\right.\\ &\left.+\delta A(F_{tzk})+\delta A(F_{fk})+\delta A(F_{sk})\right] \end{aligned} \quad (3)$$

where i = [h, m, G, w, r, at], j = [x, y, Z, r, w, d, at], k = [1, 2, …, 6]; F_r is elastic tensile force of the anchor rope, F_w is elastic bending force of the anchor winch metal structure, F_x, F_y, F_z are projections on coordinate axes x, y and z operational forces during harvester operation, F_d is viscoelastic force of the harvester head damper to reduce its rocking, F_{at} is viscoelastic force when bending an anchor tree, F_{txk}, F_{tyk}, F_{tzk} are viscoelastic forces during deformation of the k-th harvester wheel along the coordinate axes x, y and z, and F_{sk} is viscoelastic force generated by the k-th wheel suspension.

Applying eqn. 3 sequentially for all generalized possible displacements δq_i, we obtain the following calculation equations in matrix form to determine the generalized forces Q_i ($1 \le i \le 34$ – eqn. 4):

$$\{Q\}=[A]\{q\}+[B]\{\dot{q}\}+[C]\{F\}+\{D\} \quad (4)$$

where {Q}, {q}, {q̇} are vectors of generalized forces, generalized coordinates, and generalized velocities, {F} is vector of projections of operational forces on the coordinate axes, {D} is vector of constant coefficients, [A] is diagonal matrix of coefficients for generalized coordinates, [B] is the square matrix of coefficients at generalized velocities, [C] is rectangular matrix for projections of operational forces. The structure and calculation formulas for the elements of these vectors and matrices are given in Appendix 1 (Supplementary material).

Substituting eqn. 2 and eqn. 4 into eqn. 1 yields the final form of the system of motion equations characterizing the dynamics of the simulated six-component system (eqn. 5):

$$[E]\{\ddot{q}\}=\{Q\} \text{ or } \{\ddot{q}\}=\{G\} \quad (5)$$

under initial conditions (at $\tau = \tau_0 = 0$ – eqn. 6, eqn. 7):

$$\{q\}(\tau_0)=\{q_0\} \quad (6)$$

$$\{\dot{q}\}(\tau_0)=\{\dot{q}_0\} \quad (7)$$

where {q̈} is a vector of generalized accelerations, [E] is a diagonal matrix of coefficients for generalized accelerations, and {G} is a vector of the right-hand sides of the motion equations. The structure and calculation formulas for the elements of the vectors {q̈} and {G}, and the matrix [E], are given in the Supplementary Material.

Force impact on a working harvester

The force impact on the harvester during operation is not only caused by the action of weights created by the structural components of the six-component simulated system. Inertial forces that arise when the log is moved from where it was cut to where it will be stacked also play a significant role. Conditionally, they can be considered to be applied at the center of mass c.g$_{hh}$ (Fig. 1). These loads form a vector of projections of operational forces on the coordinate axes {F} in eqn. 4 when calculating the elements of the vector of generalized forces {Q}. Thus, the vector {F} is defined as (eqn. 8):

$$\{F\}=\begin{Bmatrix}F_x\\F_y\\F_z\end{Bmatrix}=\begin{Bmatrix} M_G\sin\alpha_s\cos q_{m1}\\ +\sum_i F_{c,ix}+\sum_i F_{\tau,ix}+F_{4x}+\sum_j F_{j4x}\\ gM_G\cos\alpha_s\\ +\sum_i F_{c,iy}+\sum_i F_{\tau,iy}+F_{4y}+\sum_j F_{j4y}\\ igM_G\sin\alpha_s\sin q_{m1}\\ +\sum_i F_{c,iz}+\sum_i F_{\tau,iz}+F_{4z}+\sum_j F_{j4z} \end{Bmatrix} \quad (8)$$

with $i = j$ = [1, 2, 3]. The modulus of operational forces is determined as (eqn. 9):

$$F(\tau)=[F_x^2+F_y^2+F_z^2]^{0.5} \quad (9)$$

where g is acceleration of gravity, q_{m1} is the angle of rotation of the manipulator column (link 1), $F_{c,ix}$, $F_{c,iy}$, $F_{c,iz}$ are projections on x, y and z the axes of inertial centrifugal force during rotation of the i-th manipulator rotary link, $F_{\tau,ix}$, $F_{\tau,iy}$, $F_{\tau,iz}$ are projections on x, y and z the axes of inertial tangential force during rotation of the i-th manipulator rotary link, F_{4x}, F_{4y}, F_{4z} are projections on x, y and z the axes of inertial force during linear movement of the manipulator telescopic link, F_{j4x} is the Coriolis force at the simultaneous movement of the j-th rotary link and telescopic link.

The direction and magnitude of the inertial forces are determined by the time variation laws of the kinematic parameters of the manipulator's links when moving the log. The mathematical model of the six-component system under study takes into account that, when moving the log with a motionless harvester, both joint and individual operation of the movement mechanisms of the manipulator links is possible. The model assumes that the law of change in the coordinate of the k-th motion in time $q_{mk}(\tau)$ obeys the piecewise linear law of change in the motion velocity $\dot{q}_{mk}(\tau)$ with three characteristic periods: (i) the overclocking period from rest to stationary speed ($\dot{q}_{mk} = q_{st,k}$ = const); (ii) the period of steady motion with stationary speed ($\dot{q}_{st,k}$); (iii) the braking period to a complete stop.

Solving a system of motion equations

The Runge-Kutta method of the 4th order (Schäfer 2006) was used to solve a system of ordinary differential equations of the 2nd order (eqn. 5) under initial conditions (eqn. 6, eqn. 7). The initial system of 34 ordinary differential equations of the 2nd order of the form eqn. 5, using the notation $r_i = \dot{q}_i$, is reduced to a system of 68 ordinary differential equations of the 1st order (eqn. 10):

$$\begin{cases}\{\dot{r}\}=\{G\}\\ \{\dot{q}\}=\{r\}\end{cases} \quad (10)$$

under initial conditions (eqn. 6, eqn. 11):

$$\{r\}(\tau_0)=\{r_0\}=\{\dot{q}_0\} \quad (11)$$

The solution of the equation system (eqn. 5) also serves as the basis for modeling the dynamic loading of the anchor system and evaluating the safety of its operation. These characteristics, at an arbitrary time τ, quantify parameters such as the dynamic tensile force of the anchor rope $S_r(\tau)$, the dynamic tensile stress of the anchor rope $\sigma_r(\tau)$, the strength margin factor of the anchor rope in terms of breaking force $n_r(\tau)$ and the margin factor in terms of overturning (uprooting) force on the anchor tree $n_{at}(\tau)$. They are calculated as follows (eqn. 12, eqn. 13, eqn. 14, eqn. 15):

$$S_r(\tau)=S_{r0}+c_r[\varepsilon_{at}q_{34}(\tau)-q_{32}(\tau)] \quad (12)$$

$$\sigma_r(\tau)=S_r(\tau)/f_r \quad (13)$$

$$n_r(\tau)=[T_r]/\sigma_r(\tau) \quad (14)$$

$$n_{at}=F_{at}(d_{tr},H_{tr})/S_r(\tau)\cos\psi_L \quad (15)$$

where S_{r0} is the pre-tensioning force of the anchor rope (at the initial moment of time τ_0), ε_{at} is the relative displacement of the longitudinal axis of the anchor tree, in the section where the anchor rope attaches to it, f_r, $[T_r]$ are the total cross-sectional area of the wires and the breaking force of the anchor rope (Feyrer 2015), $F_{at}(d_{tr}, H_{tr})$ is the critical overturning (uprooting) force of an anchor tree depending on its diameter d_{tr}, height H_{tr} and soil condition, ψ_L is the inclination angle of the anchor rope longitudinal axis to the coordinate axis x at the point L of its attachment to the anchor tree (Lagerev & Lagerev 2020).

Results

The mathematical model of the six-component system was implemented in the computer program "Dynamics of a harvester with an anchor rope for logging on a steep slope".

To analyze the influence of the main technical characteristics of the harvester and anchor system on the dynamic parameters of the "harvester – manipulator - anchor system - natural anchor – log - soil" system, we chose a variant of a 6-wheel harvester with an uncut frame. The main technical characteristics of the simulated harvester are shown in Tab. 1.

The calculated manipulator motion was assumed to consist of individual link movements, simulating the process of moving a log from the cutting site to the temporary stacking site. The cutting site is located along the longitudinal axis of the harvester, which corresponds to the x-axis. The stacking site is located along the transverse axis, which corresponds to the z-axis. The movements are performed in the following order: (i) lifting the boom (link 2) from the initial lower position; (ii) turning the column (link 1) from the initial longitu-

Tab. 1 - The main technical characteristics of the simulated harvester.

Technical characteristics	Designation	Value
Harvester total mass (kg)	M_h	20,000
Length/width of the harvester frame (m)	L_f/ D_f	7.8/2.0
Harvester track width (m)	D_h	2.6
Installation dimensions of the harvester axes (m)	x_{t1} / x_{t2} / x_{t3}	3.8/1.9/-0.9
Manipulator mass (kg)	M_m	2100
Length of the manipulator links (m)	L_1/L_2/L_3/L_4	1.0/4.9/3.4/1.4
Harvester head mass (kg)	M_{hh}	1 500
Distance from the harvester to the anchor tree (m)	L_r	30
Anchor rope diameter (mm)	d_r	15
Breaking force of the anchor rope (kN)	T_r	137
Preliminary tensile force of the anchor rope (kN)	S_{r0}	10
Height/diameter of the anchor tree (m)	H_{at}/D_{at}	26/0.4
Log length (m)	l_{tr}	6
Density of the log wood (kg m^{-3})	ρ_{tr}	400
Inclination angle of the ground surface (deg)	a_s	30
Wheel slip	μ_{gr}	0.4

Tab. 2 - The parameters of the movement of the manipulator links when moving the log. The asterisk (*) indicates the unit of measurement for the parameter of the telescopic link (link 4).

Parameter	Parameter value			
	link 1	link 2	link 3	link 4
Time of the start/end of the movement (s)	1.0/7.0	0 /3.8	3.0 /7.3	2.0 /8.0
Coordinate of the link at the initial/final moment (degree) or (m)*	0 /90	10 /40	60 /0	0 /1.0
Steady motion speed (deg s^{-1}) or (m s^{-1})*	40	10	20	0.2
Acceleration during overclocking/braking (deg s^{-2}) or (m s^{-2})*	10 /-10	10 /-20	15 /-15	0.2 /-0.2
Overclocking/braking time (s)	3.0/3.0	1.0 /0.5	1.3 /1.3	1.0 /1.0

Tab. 3 - Ranges of oscillation of main dynamic parameters of the simulated harvester.

Parameter	Minimum	Maximum
Movement of the center of mass of harvester along the x axis (mm)	-0.9	0.5
Movement of the center of mass of harvester along the y axis (mm)	-15.3	0.0
Movement of the center of mass of harvester along the z axis (mm)	-35.3	-0.4
Turning of the harvester around the z axis (degree)	-14.8	3.7
Movement of the center of mass of manipulator along the x axis (mm)	-5.5	1.8
Movement of the center of mass of manipulator along the y axis (mm)	-10.2	32.5
Movement of the center of mass of harvester head along the x axis (mm)	-11.7	12.5
Movement of the center of mass of harvester head along the y axis (mm)	-13.7	9.5
Movement of the winch shell along the x axis (mm)	-12.5	2.4
Movement of the center of mass of anchor tree along the x axis (mm)	-1.9	1.7
Tensile force in the anchor rope (kN)	13.2	19.5
Axial tensile stress in the anchor rope (MPa)	153.2	226.1
Strength margin factor of the anchor rope in terms of breaking force	7.0	10.4
Margin factor for the overturning force on the anchor tree	2.1	3.1

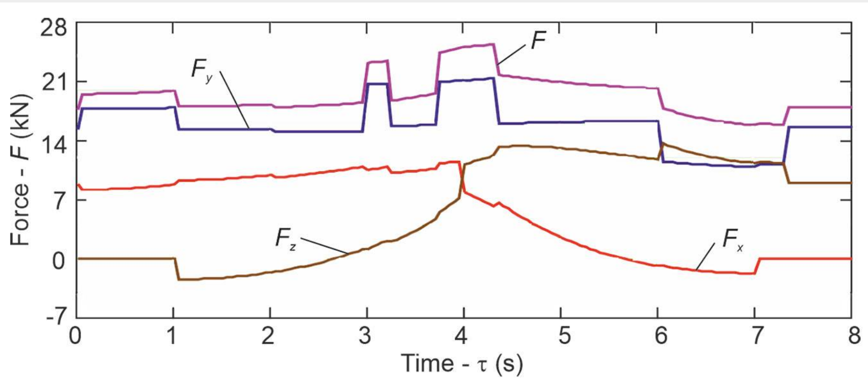

Fig. 2 - The time variation of the forces acting on the harvester head.

dinal position; (iii) extending the telescopic link (link 4) from the initial maximum pushed position; (iv) lowering the handle (link 3) from the initial upper position.

The parameters of each link's movement during the process of moving the log are presented in Tab. 2.

Fig. 2 shows the time-dependent graphs of the module and the projections of the operational forces onto the coordinate axes as the log is moved. The greatest values of these forces are observed approximately in the time interval between 3.7 and 4.3 seconds, which corresponds to when three links are in motion – rotary links 1 and 3 and telescopic link 4.

Tab. 3 presents the quantitative results of dynamic calculations for the harvester's basic option and its anchor system during log movement. These results characterize the ranges of oscillations in the main dynamic parameters. Fig. S3 to Fig. S5 (Supplementary material) illustrate the dynamics of these key parameters. As the time step used for integrating the system of differential equations (eqn. 5) was 0.1 milliseconds, these figures present the calculated results for four time intervals of 0.05 seconds each: (i) the initial period of the manipulator operation is from 0.50 to 0.55 seconds, when only the boom (link 2) performs the rotary movement; (ii) the period from 3.20 to 3.25 seconds, when all four links of the manipulator move together; (iii) the period from 4.1 to 4.15 seconds, in which the maximum operational load on the harvester head is observed and three links are moving together, *i.e.*, the column (link 1), the handle (link 3), and the telescopic link (link 4); (iv) the final period of the manipulator operation is from 7.50 to 7.55 seconds, when only the telescopic link (link 4) performs the movement.

A quantitative analysis of the graphs in Fig. S3 to Fig. S5 (Supplementary material) showed that the oscillation periods of the studied characteristics are independent on operating loads and do not change during log movement. They are determined by geometric dimensions of structural elements of a simulated dynamic system. The approximate oscillation frequencies of the dynamic characteristics of the anchor rope (S_r, σ_r, n_r, n_{at}) and the displacement of the center of mass of the anchor winch q_{32} are approximately 1.8 kHz. The oscillation frequency of the center of mass of the harvester head q_{10} is approximately 5 kHz. The dynamics of the center-of-mass movement of the anchor tree q_{34} have a distinctive feature. High-frequency vibration at 5.3 kHz and low-frequency vibration at 440 Hz can be clearly observed.

A visual analysis of the dynamic processes in Fig. S3 to Fig. S5 (Supplementary material) revealed that the investigated parame-

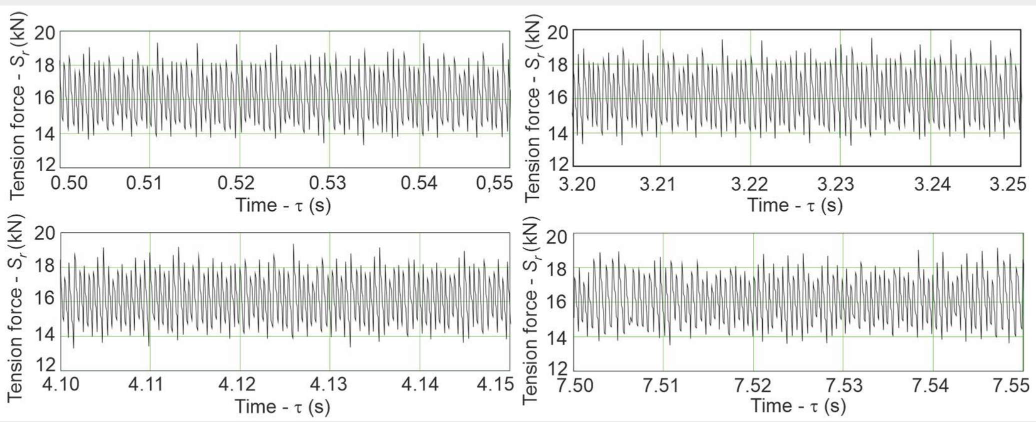

Fig. 3 - The dynamics of the anchor's rope tensile force.

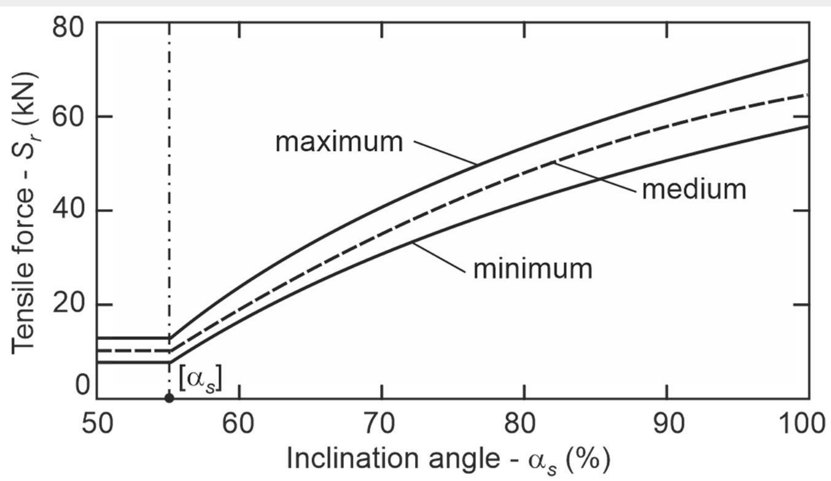

Fig. 4 - Influence of the inclination angle of the support surface on the tensile force of the anchor rope.

ters of the harvester and its anchor system exhibit a variable range during the log moving. The magnitude of this range is defined as the difference between the two adjacent extremes of a given *k*-th parameter, as shown in eqn. 16:

$$\Delta U_k = |U_{k,extr,2} - U_{k,extr,1}| \quad (16)$$

where $U_{k,extr,1}$ and $U_{k,extr,2}$ are values of the previous and subsequent extreme points of the dynamic process.

To quantify the magnitude of the oscillations in the parameters of the harvester basic option, histograms were generated to show their distributions over the range between the minimum and maximum values ($\Delta U_{k,min}$ and $\Delta U_{k,max}$, respectively). These histograms are presented in Fig. S6 (Supplementary material). A comparison of the histograms for characteristic time intervals with the level of operational load in those same time intervals (Fig. 2) leads to the following conclusion: as the load increases, the ranges of the parameters S_r, σ_r, n_r, and n_{at} also increase, and their values become more consistent and have a narrower spread.

Discussion

In this study, we present, for the first time, an approach to modeling the dynamic behavior of a wheeled harvester with an anchor rope system, using a winch and an anchor tree. This approach is based on a complex mathematical model that includes six components: harvester, manipulator, anchor system, natural anchor, log, and soil. This approach enables combining all the key components of the phenomenon under study into a single model and evaluating their mutual influence on the quantitative parameters of ongoing dynamic processes. Using this model requires specifying a significant amount of source data. These can be roughly divided into groups, such as: (i) structural dimensions, weight, and mechanical properties of the main structural components of the harvester and anchor system; (ii) dimensions and physical properties of anchor trees; (iii) geometric parameters of the slope and physical and mechanical properties of the support surface; (iv) operating parameters during harvester operation, which determine the kinematics of log movement and the time change in the load level of the structural components of the harvester and rope anchor system.

The key characteristic of the dynamic behavior of the harvester's rope anchor system is the dynamic tensile force of the anchor rope $S_r(\tau)$. It is determined by eqn. 12, based on the pre-tensioning force of the anchor rope S_{ro} and the elongation of the anchor rope calculated for the moment of time τ. The tensile force of the anchor rope exhibits an oscillatory pattern (Fig. 3), with its amplitude and extreme values increasing as the slope becomes steeper. An analysis of the graphs in Fig. 2 leads us to conclude that the main cause of the dynamic behavior of the tensile force in the anchor rope during operations is the time-varying inertial force due to the acceleration of moving logs. For the simulated harvester, the change in the tensile force with increasing slope steepness is shown in Fig. 4. The maximum values of the force in the studied range of slope steepness increased from 19 to 72 kN, while the average values increased from 16 to 65 kN, with an increase in the range of oscillation from 6 to 14 kN.

Such a change in the tensile force of the anchor rope over time during the operation of forestry machinery is confirmed by well-known field research of various types of harvesters and forwarders in different operating conditions on steep slopes (Holzleitner et al. 2018, Mologni et al. 2018, 2021a, 2021b). The dependence of the support surface inclination angle on the tensile force of the anchor rope is also qualitatively consistent with the findings of the same studies.

An objective quantitative comparison between the modeling results for the anchor rope tensile force and the data derived from these studies is infeasible due to insufficient information required to apply the developed mathematical model. However, given that the simulation was conducted for a real-world harvester, it is possible to make a rough comparison between the real and simulated data. The data presented by Mologni et al. (2021b) are the most suitable for such a comparison. During the work of felling and storing trees using a CAT 552-2 tracked harvester weighing 38 tons on slopes up to 77%, the average tensile forces in the anchor rope ranged from 70 to 77 kN, with maximum values ranging from 130 to 137 kN. Our simulated data (Fig. 4) with the same slope are 52 and 59 kN, respectively.

As shown in Fig. 4, for a slope steepness lower than 55% (< 29 degrees), the tensile force remains constant, although it fluctuates within a range of 4 kN. When the slope steepness exceeds 55%, the tensile force increases. Thus, the breaking point of the $S_r(\alpha_s)$ curve defines the threshold for the slope steepness α_s. Above this boundary, the mandatory use of a rope anchor system is necessary to ensure the stability and safety of the harvester during tree felling operations. The value $\alpha_s \approx 55\%$, obtained using the developed mathematical model, is consistent with data reported in the literature (Berkett & Visser 2012, Holzfeind et al. 2020, Visser & Spinelli 2023). The value α_s is mainly influenced by the total weight of the harvester, the slip coefficient of the wheels on the soil, and the pre-tensioning force of the anchor rope. It increases as these characteristics increase. Therefore, it is a value that can change for the same harvester when it operates in different cutting areas with different pre-tensioning of the anchor rope.

As shown by the simulation results, pre-tensioning the anchor rope before the beginning of harvester operations improves the maximum inclination angle of the supporting surface. However, this leads to a non-linear increase in the average and maximum values of the total anchor rope tension. This finding is qualitatively consistent with the results of the research by Visser & Stampfer (2015).

Other characteristics of interest of the dynamic behavior, such as $\sigma_r(\tau)$, $n_r(\tau)$ and $n_{at}(\tau)$, are uniquely determined by the force $S_r(\tau)$. This is because, according to eqn. 13 and eqn. 14, these characteristics are different from $S_r(\tau)$ by a constant factor.

Obviously, the minimum values of the strength margin factor of the anchor rope in terms of breaking force $n_{r,min}$ and the margin factor for the overturning force on the anchor tree $n_{at,min}$, which are determined by the maximum values of the rope tension $S_{r,max}$, determine the conditions for harvester safe operation on the slope. These conditions are expressed by inequalities (eqn. 17, eqn. 18):

$$n_{r,min} = f_r[T_r] / S_{r,max} \geq [n_r] \quad (17)$$

$$n_{at,min} = F_{at} / S_{r,max} \cos\psi_L \geq [n_{at}] \quad (18)$$

where $[n_r]$, $[n_{at}]$ are normative margin factors, which are established by technical regulations that ensure the safety of harvester operation.

When harvesters are operating on steep slopes, there is a change in the magnitude of the load acting on the mechanisms of movement of the manipulator's links during the spatial movement of the log. Experimental studies by Mergl & Kašpárek (2022) showed that with an increase in the inclination of the manipulator rotary mechanism caused by the location of the harvester on an inclined support surface, more lifting torque is required to manipulate logs of the same weight. This is most evident in the longitudinal plane of the machine when working downhill. Simulated calculations also produce similar results: when the slope increases from 27% to 100% (or from 15 degrees to 45 degrees), the lifting moment increases by approximately 30%.

Conclusions

The dynamic mathematical 12-mass model presented in this study integrates all the key components of the simulated phenomenon into a single, interconnected system. This includes the harvester itself, with a manipulator and harvester head attached, a moving log in space, an anchor system consisting of an anchor rope and winch, and an anchor tree for fastening the anchor rope to the soil of the support surface.

As a result, this dynamic model of the six-component "harvester - manipulator - anchor system - natural anchor - log - soil" system enables mathematical modeling of workflows for a three-axle wheeled harvester with an uncut machine frame operating on a steep slope during log movement. The proposed approach could similarly be extended to harvesters with a different number of wheels, different design features (for example, the frame structure), and different types of natural and artificial anchors (including stumps or recessed metal rods). As a result, a promising avenue for future research is adapting the dynamic model for the six-component system, as proposed in this work, to other variants of modern harvester designs, including tracked harvesters. A more in-depth modification of the proposed dynamic model would also be desirable, focusing on the complex modeling of work processes for forwarders equipped with rope-anchoring systems based on retaining winches.

The dynamic model enabled a systematic analysis of a large number of quantitative structural and regime parameters, as well as the physical and mechanical properties of soils. These parameters characterize the dynamic behavior and loading of the harvester and the manipulator mounted on it, as well as the structural elements of the anchor system. Thus, the developed dynamic model can serve as a mathematical tool for both quantitative and qualitative assessment of the impact of individual parameters, or several parameters simultaneously, on the dynamic behavior of harvesters. This information will be of great practical importance in the design of rope anchor systems, which provide the necessary stability and safety for harvesters operating on steep slopes. As a result, the obvious direction for further research is to determine qualitative and quantitative relationships between characteristic sizes, technical characteristics of harvesters, their anchor systems, operating modes, soil properties, and cutting area characteristics, with key parameters for safe operation – permissible inclination angles of support surfaces, ranges of dynamic tensile force variations in anchor ropes, optimal pre-tensions of anchor rope, sizes of suitable anchor trees, etc. The analysis of these relationships can serve as a basis for developing practical recommendations at both the design stage of specialized equipment and its operational stage. At the design stage, they will ensure the development of anchor equipment that meets the customer-defined conditions for subsequent operations. These recommendations will allow us to reasonably select anchoring equipment with parameters that can reliably ensure the operation of forestry machinery, based on the specific conditions in the cutting areas.

Acknowledgements

AL proposed the research topic and completed the preparation of the manuscript's final version; AL, IL, and AM participated in the development of a mathematical model and the evaluation of its correctness; IL developed and tested the computer program; AM performed calculations and analyzed the results. All authors read and approved the final manuscript.

References

Aggestam F, Konczal A, Sotirov M, Wallin I, Paillet Y, Spinelli R, Lindner M, Derks J, Hanewinkel M, Winkel G (2020). Can nature conservation and wood production be reconciled in managed forests? A review of driving factors for integrated forest management in Europe. Journal Environmental Management 268: 9. - doi: 10.1016/j.jenvman.2020.110670

Belart F, Leshchinsky B, Chung W (2025). Characterization of ground pressure at different cable tension on tether-assist tracked self-leveling feller-buncher. Journal of Forestry 123: 161-170. - doi: 10.1007/s44392-024-00002-z

Berkett H, Visser R (2012). Measuring slope of forestry machines on steep terrain. Harvesting Technical Note HTN05-02, Future Forests Research Limited, Rotorua, New Zealand, pp. 7. [online] URL: http://www.researchgate.net/publication/371124850

Bont L, Heinimann H (2012). Optimum geometric layout of a single cable road. European Journal of Forest Research 131 (5): 1439-1448. - doi: 10.1007/s10342-012-0612-y

Breinig L, Hinte B, Schönauer M, Hoffmann S, Brokmeier H, Jaeger D (2025). Traction assistance of a forwarder in flat terrain: effects on wheel slip and soil disturbance. Croatian Journal of Forest Engineering 46 (1): 1-17. - doi: 10.5552/crojfe.2025.2434

Ceccarelli M (2008). Robot manipulators. In-Tech, Vienna, Austria, pp. 546. [online] URL: http://books.google.com/books?id=XwWQDwAAQBAJ

Di Fulvio F, Acuña M, Ackerman P, Ackerman S, Spinelli R, Abbas D, Kaakkurivaara N, Sánchez-García S, Guerra SPS (2024). Benchmarking operational conditions, productivity, and costs of harvesting from industrial plantations in different global regions. International Journal of Forest Engineering 35 (2): 225-250. - doi: 10.1080/14942119.2023.2296789

Duka A, Papa I, Proto A, Latterini F, Mederski P, Borz S, Iordache E, Sokolovic D, Karisik A, Stojnic D, Danilovic M, Picchio R (2025). Forest accessibility and road network density: a global overview with a special focus on Europe. Current Forestry Reports 11: 26. - doi: 10.1007/s40725-025-00259-3

Feyrer K (2015). Wire ropes. Tension, endurance, reliability. Springer-Verlag, Berlin, Heidelberg, Germany, pp. 336. - doi: 10.1007/978-3-642-54996-0

Green P, Chung W, Leshchinsky B , Belart F, Sessions J (2020). Insight into the productivity, cost and soil impacts of a cable-assisted harvester-forwarder thinning in western Oregon. Forest Science 66 (1): 82-96. - doi: 10.1093/forsci/fxz049

Grigorev I, Burgonutdinov A, Makuev V, Tikhonov E, Shvetsova V, Timokhova O, Revyako S, Dmitrieva N (2022). The theoretical modeling of the dynamic compaction process of forest soil. Mathematical Biosciences and Engineering 19 (3): 2935-2949. - doi: 10.3934/mbe.2022135

Grim D (2025). Winch assist systems for steep slope logging. TimberWest Magazine 3. [online] URL: http://forestnet.com/winch-assist-systems-for-steep-slope-logging/

Holzfeind T, Visser R, Chung W, Holzleitner F, Erber G (2020). Development and benefits of winch-assist harvesting. Current Forestry Reports 6: 201-209. - doi: 10.1007/s40725-020-00121-8

Holzleitner F, Kastner M, Stampfer K, Höller N, Kanzian C (2018). Monitoring cable tensile forces of winch-assist harvester and forwarder operations in steep terrain. Forests 9 (2): 53-65. - doi: 10.3390/f9020053

Humphrey P, Harvey C, Visser R (2024). Deploying an early-stage cyber-physical system for the implementation of Forestry 4.0 in a New Zealand timber harvesting context. iForest - Biogeosciences and Forestry 17: 353-359. - doi: 10.3832/ifor4651-017

Ismoilov A, Sellgren U, Pirnazarov A, Anderson K, Löfgrenb B (2014). Investigating the dynamic behavior of a mid-sized forestry machine on sloped rough terrain. In: Proceedings of the "18th International Conference of the International Society for Terrain Vehicle Systems". Seoul (Korea) 22-25 Sept 2014. Curran Associates, New York, USA, pp. 1-8. [online] URL: http://www.researchgate.net/publication/282736125

Kormanek M, Dvorák J, Tylek P, Jankovsky M, Nuhlícek O, Mateusiak L (2023). Impact of MHT9002HV tracked harvester on forest soil after logging in steeply sloping terrain. Forests 14 (5): 977-988. - doi: 10.3390/f14050977

Kovác J, Gregor I, Melichercík J, Kuvik T (2023). Analysis of the operating parameters of wood transport vehicles from the point of view of operational reliability. Forests 14 (7): 1511-1522. - doi: 10.3390/f14071511

Lagerev AV, Lagerev IA, Milto AA (2014). Tool for preliminary dynamics and stress analysis of articulating cranes. International Review of Modeling and Simulation 7 (4): 644-652. - doi: 10.15866/iremos.v7i4.2045

Lagerev AV, Lagerev IA (2020). Designing supporting structures of passenger ropeways of minimum cost based on modular intermediate towers of discretely variable height. Urban Rail Transit 6 (4): 265-277. - doi: 10.1007/s40864-020-00137-0

Lagerev AV, Lagerev IA, Makulina AV (2025). Improving the harvester functionality by optimizing the manipulator kinematic scheme. iForest - Biogeosciences and Forestry 18 (4): 227-233. - doi: 10.3832/ifor4753-018

Leschinsky B, Sessions J, Wimer J (2015). Analytical design for mobile anchor systems. International Journal of Forest Engineering 26 (1): 10-23. - doi: 10.1080/14942119.2015.1023014

Lyons CK, Sessions J, Wimer J (2020). Design of continuous bridle multiple-stump anchors. International Journal of Forest Engineering 31 (1): 1-8. - doi: 10.1080/14942119.2020.1685833

Machuga O, Shchupak A, Styranivskiy O (2024). Field and laboratory research of the rut development process on forest roads. Forests 15 (1): 74-90. - doi: 10.3390/f15010074

Marchi L, Mologni O, Trutalli D, Scotta R, Cavalli R, Montecchio L, Grigolato S (2019). Safety assessment of trees used as anchors in cable-supported tree harvesting based on experimental

observations. Biosystems Engineering 18: 71-82. - doi: 10.1016/j.biosystemseng.2019.06.022
McEwan A, Marchi E, Spinelli R, Brink M (2020). Past, present and future of industrial plantation forestry and implication on future timber harvesting technology. Journal of Forest Research 31 (2): 339-351. - doi: 10.1007/s11676-019-01019-3
Mergl V, Kašpárek J (2022). Verifying the lifting and slewing dynamics of a harvester crane with possible levelling when operating on sloping grounds. Forests 13 (2): 357-376. - doi: 10.3390/f13020357
Meyers M, Chawla K (2009). Mechanical behavior of materials. Cambridge University Press, Cambridge, UK, pp. 882. - doi: 10.1108/aeat.2009.12781bae.001
Mologni O, Dyson P, Amishev D, Proto A, Zimbalatti G, Cavalli R, Grigolato S (2018). Tensile force monitoring on large winch-assist forwarders operating in British Columbia. Croatian Journal of Forest Engineering 39 (2): 193-204.
Mologni O, Lyons C, Marchi L, Amishev D, Grigolato S, Cavalli R, Roser D (2021a). Assessment of cable tensile forces in active winch-assist harvesting using an anchor machine configuration. European Journal of Forest Research 140: 745-759. - doi: 10.1007/s10342-020-01347-8
Mologni O, Nance E, Lyons C, Marchi L, Grigolato S, Cavalli R, Roeser D (2021b). Cable tensile forces associated to winch design in tethered harvesting operations: a case study from the Pacific North West. Forests 12: 827. - doi: 10.3390/f12070827
Molotnikov V, Molotnikova A (2023). Theoretical and applied mechanics. Springer, Cham, Switzerland, pp. 684. - doi: 10.1007/978-3-031-09312-8
Naillon T, Rappin C (2019). Best management and operating practices for steep slope machine logging. Technical Report no. 98-02-2019, Washington State Department of Labor and Industries, Safety and Health Assessment and Research for Prevention (SHARP) Program, Washington, DC, USA, pp. 43.
Papadopoulos E, Sarkar S (1997). The dynamics of an articulated forestry machine and its applications. In: Proceedings of the "IEEE International Conference on Robotics and Automation". Albuquerque (NM, USA) 20-25 Apr 1997. Piscataway, NJ, USA, pp. 323-328. - doi: 10.1109/ROBOT.1997.620058
Placet V, Passard J, Perre P (2007). Viscoelastic properties of green wood across the grain measured by harmonic tests in the range 0-95 degrees C: hardwood *vs.* softwood and normal wood *vs.* reaction wood. Holzforschung 61 (5): 548-557. - doi: 10.1515/HF.2007.093
Pracejka HB (2006). Tire and vehicle dynamics. Elsevier Ltd, Oxford, UK, pp. 620.
Schäfer M (2006). Computational engineering - Introduction to numerical methods. Springer-Verlag, Berlin Heidelberg, Germany, pp. 321. - doi: 10.1007/3-540-30686-2_2
Sessions J, Leshchinsky B, Chung W, Boston K, Wimer J (2017). Theoretical stability and traction of steep slope tethered feller-bunchers. Forest Science 63 (2): 192-200. - doi: 10.5849/forsci.16-069
Shoop SA (2001). Finite element modeling of tire-terrain interaction. Technical Report ERDC/CRREL TR-01-16, Cold Regions Research and Engineering Laboratory, Hannover, Germany, pp. 59.
Siciliano B, Khatib O (2016). Springer handbook of robotics. Springer-Verlag, Berlin Heidelberg, Germany, pp. 2227. - doi: 10.1007/978-3-319-32552-1
Sun J, Meng C, Zhang Y, Chu G, Zhang Y, Yang F, Liu Z (2020). Design and physical model experiment of an attitude adjustment device for a crawler tractor in hilly and mountainous regions. Information Processing in Agriculture 7 (3): 466-478. - doi: 10.1016/j.inpa.2020.02.004
Vereecken H, Schnepf A, Hopmans JW, Javaux M, Roose DOT, Vanderborght J (2016). Modeling soil processes: review, key challenges, and new perspectives. Vadose Zone Journal 15: 1-57. - doi: 10.2136/vzj2015.09.0131
Vinogradov OG (2000). Fundamentals of kinematics and dynamics of machines and mechanisms. CRC Press, Boca Raton, FL, USA, pp. 290. [online] URL: http://books.google.com/books?id=HbC2p6aW2e0C
Visser R, Raymond K, Harrill H (2014). Developing fully mechanised steep terrain harvesting operations. In: Proceedings of the "47th International Symposium on Forestry Mechanisation". Gerardmer (France) 23-26 Sept. 2014. FORMEC, France, pp. 1-8.
Visser R, Stampfer K (2015). Expanding ground-based harvesting onto steep terrain: a review. Croatian Journal of Forest Engineering 36 (2): 321-331.
Visser R, Spinelli R (2023). Benefits and limitations of winch-assist technology for skidding operations. Forests 14: 296. - doi: 10.3390/f14020296
Wassermann C (2018). Mastseilgerate fur die Holzernte: Eine Analyse des europaischen Herstellerangebotes [Mast rope devices for timber harvesting: an analysis of the European manufacturer's offer]. Master's thesis, University of Natural Resources and Life Sciences, Vienna, Austria, pp. 110. [in German]

Supplementary Material

Appendix 1 - The structure and values of the elements in vectors and matrices that form the system of motion equations.

Fig. S1 - Geometric model.

Fig. S2 - Generalized coordinates of the dynamic mathematical model.

Fig. S3 - The dynamics of the mass center movement of an anchor tree.

Fig. S4 - The dynamics of the anchor winch drum's movement.

Fig. S5 - Dynamics of the mass center movement of the harvester head and the log along the *x*-axis.

Fig. S6 - Histograms of the distribution of the ranges of relative share for the anchor's rope tensile force (a), the mass center movement of the harvester head and the log along the *x*-axis (b), the anchor winch drum's movement (c), and the mass center movement of an anchor tree (d).

Link: Lagerev_4983@suppl001.pdf